Bound substitutional impurity pairs in diamond: a density functional study

2008 J. Phys.: Condens. Matter 20 085217

(http://iopscience.iop.org/0953-8984/20/8/085217)

J. Phys.: Condens. Matter **20** (2008) 085217 (9pp) doi:10.1088/0953-8984/20/8/085217

Bound substitutional impurity pairs in diamond: a density functional study

J P Goss, R J Eyre and P R Briddon

School of Natural Sciences, University of Newcastle upon Tyne, Newcastle upon Tyne, NE1 7RU, UK

E-mail: J.P.Goss@ncl.ac.uk

Received 12 September 2007, in final form 7 December 2007
Published 1 February 2008
Online at stacks.iop.org/JPhysCM/20/085217

Abstract

Substitutional nitrogen and boron are known to form nearest-neighbour pairs in diamond, leading to donor and acceptor levels deep within the band-gap relative to the isolated counterparts. For n-type doping, even isolated nitrogen donors possess very deep levels, and thus larger impurities are used. With species such as phosphorus and sulfur, elastic repulsion might be expected to prevent donor aggregation seen for the smaller dopant species. However, we show from density functional simulations that large impurities can form additional chemical interactions when in close proximity, rendering them energetically bound. These direct, localized interactions produce localized electrical levels deep in the band-gap, rendering them inactive for electrical conduction, and possibly optically active. As a consequence, pairing of P, S and other species in heavily doped and/or high-temperature annealed material would impact upon electrical activation of dopants.

(Some figures in this article are in colour only in the electronic version)

1. Introduction

Doping diamond for electronic applications has proved a challenge, partly due to low dopant solubility for most chemical species, and partly due to the deep levels that result from their incorporation.

Boron has an acceptor level at around 0.37 eV [1], dropping towards the valence band top (E_v) with increasing concentration [2]. For n-type diamond the challenge is greater. Nitrogen and phosphorus yield deep donor levels [3, 4] at $E_c - 1.7$ eV and $E_c - 0.6$ eV, respectively (E_c representing the conduction band minimum), and although sulfur doping has also shown promise [5–9], most quantum-mechanically based modelling suggests substitutional sulfur (S_s) possesses a deep donor level [10–20].

Substitutional arsenic theoretically possesses a shallow level [17, 21], but to-date As-doping has only been achieved using ion implantation which is beset by compensating implantation damage [22].

The lack of practical doping using traditional methods has lead to suggested shallow donors resulting from heterogeneous co-doping [12, 23, 24], but the efficacy of these complex systems seems doubtful [21, 25, 26].

Perhaps a more plausible multi-component donor would be nearby pairs of donors of the same chemical species. Indeed, in silicon chalcogen pairs yield shallower donor levels than isolated S, Se, and Te [27]. This may be understood in terms of overlapping donor states in even and odd combinations, as shown schematically in figure 1(a). Here the odd combination is pushed up in energy, rendering the chalcogen pairs shallow donors.

Figure 1(b) shows the corresponding simple case for single donors. Here one expects deeper donor levels, and indeed, this reflects the case of two nitrogen donors in diamond, where the occupied band lies closer to E_v than E_c [19, 28].

We have previously examined a range of impurity complexes using quantum-mechanically based methods [26]. These show that the simplistic model presented in figure 1 is not generally applicable to impurity pairs. For a particularly technologically relevant example, phosphorus and arsenic pairs on adjacent sites possess donor levels close the substitutional phosphorus (P_s) marker level at $E_c - 0.6$ eV, but on second-neighbour sites yield much deeper donor levels at $E_c - 2.0$ eV and $E_c - 1.5$ eV, respectively. This is in contrast to what one would expect from figure 1(b): if the donor level of a P-pair arose from simple odd and even combinations of single

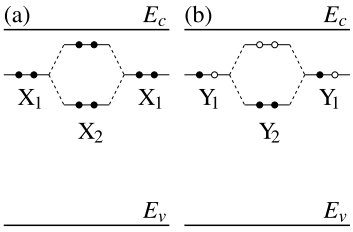

Figure 1. Schematic of the interaction of levels associated with (a) double donors (X) and (b) single donors (Y). In each case the interaction between two single centres is assumed to lead to even and odd combinations of donor states, the latter being pushed toward the conduction band. Black and white circles represent filled and empty states, respectively.

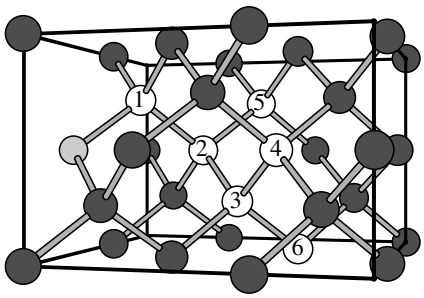

Figure 2. Schematic showing in white the six nearest sites to the light grey atom in a diamond structure material.

donor states, the donor level should be deepest for nearest-neighbour pairs, and rise toward E_c as the distance increases and the interaction is reduced, converging to the value of isolated phosphorus donors.

Our previous calculations [26] also indicate a second property for impurity pairs made up from large atomic species: they are energetically bound. For example, phosphorus and sulfur donors are more stable in second-neighbour pairs than in adjacent pairs, consistent with the repulsive strain expected for these large impurities. However, the second-neighbour pairs are also lower in energy than two isolated donors, indicating that the elastic strain is being overcome by an attractive interaction between the donors.

Given the unexpected binding of large dopants on close-by sites, and since such species are important for the development of n-type diamond, we have extended our earlier study [26] to help develop a better understanding of the properties particularly of donor-pair systems. In this paper we explore the stability of impurity pairs and the implications for electrical activity.

2. Method

Calculations were carried out using the local-spin-density-functional technique, implemented in AIMPRO [29], using the PW92 [30] functional.

To model the defects, 216 atom, cubic supercells of side length $3a_0$ have been used. The Brillouin-zone is sampled using the Monkhorst–Pack scheme [31], generally with a mesh of $2 \times 2 \times 2$ special k-points, with convergence checked by calculating total energies with denser meshes for selected systems. Core-electrons are eliminated by using norm-conserving pseudo potentials [32].

Impurity pairs have been analysed for the six nearest sites shown in figure 2. It is important to minimize the interaction of defects with their periodic images. In particular, for site 6 in figure 2 using the 216 host-atom supercell, the grey atom is at $[112]a_0/2$, and its nearest image at $[411]a_0/2$. The difference is deemed sufficient to describe the simulations as isolated impurity pairs. Relaxation is performed using a conjugate-gradients algorithm, terminated where incremental energy changes are less than 0.3 meV. Structures were obtained with symmetry constraints where appropriate, and subsequently re-relaxed where the atoms were displaced in random directions by $\sim$0.1 Å to avoid artificial minima.

The activation energies for conversion between geometries are calculated via the climbing nudged-elastic-band method (the so-called NEB technique) [33, 34], using a minimum of nine images.

The wavefunction basis consists of atom-centred Gaussians [35]. Carbon atoms are treated using linear combinations of s- and p-orbitals with the addition of a set of d-functions to allow for polarization. This amounts to 13-basis functions per C atom. Impurities are treated using four independent sets of s- and p-Gaussians with the addition of four sets of d-polarisation functions, resulting in 40 basis functions per impurity atom. The charge density is Fourier transformed using plane-waves with a cut-off of 350 Ryd, yielding well converged total energies.

Using the above procedure, the lattice constant and bulk modulus of bulk diamond are reproduced to within $\sim$1 and 5% respectively of experiment, while the direct and indirect band gaps at 5.68 eV and 4.26 eV, respectively, are close to previously published plane-wave values [36]. However, these values are underestimates of the experimental values, with the measured indirect gap of 5.48 eV [37]. The underestimate of the band-gap affects calculations involving the location of levels (both optical and electrical) within the band-gap. In the case of optical transitions we therefore restrict ourselves to qualitative analysis, but for electrical transitions the impact of the error in the band-gap is reduced by use of the marker-method, which we describe below. Regardless of the quantitative accuracy of the donor and acceptor levels, whether pairing impurities leads to shallower or deeper levels is much less dependent upon the error in the band-gap, and qualitatively the results presented here are likely to be correct.

We define a binding energy by $E^{\mathrm{b}}(X_2) = E^f(X_2) - 2E^f(X)$. In the current data set, the binding energies are established by comparison with the total energies for pairs separated as far as possible within the supercell. This is the sixteenth nearest shell in the pure lattice, with an inter-nuclear separation of $[233]a_0/2$.

Band structures diagrams are produced by first obtaining the self-consistent charge density and potential using a $2\times2\times2$ Monkhorst–Pack mesh. The Kohn–Sham spectra at k-points along high-symmetry directions within the first Brillouin-zone are then obtained using this potential.

Electrical levels are estimated using the marker-method [35]. This involves the calculation of the ionization energies for the system under analysis (D), as well as some other similar system for which the level is known experimentally (the marker, M). Then, for example a donor level is obtained by calculating

$$\Delta E = \{E(D, 0) - E(D, 1+)\} - \{E(M, 0) - E(M, 1+)\},$$

the difference in the calculated ionization energies where $E(X, q)$ is the total energy of system X in charge state q. Since $E(M, 0) - E(M, 1+)$ is the experimental reference point, this locates the donor level of D relative to the band-gap. Similar expressions exist for other electrical transitions. Since ΔE may be written as differences in total energies for systems with the same charge state, this approach mitigates the well known problems associated with calculating the properties of charged systems within periodic boundary conditions. This can be viewed as a cancellation of systematic errors, since the error in the total energy of charged systems due to the periodic boundary condition in its simplest form is a function of the cell size and the charge state only [38]. Where the point-charge approximation is valid, the relative ionization energy of two systems is independent of the Makov–Payne Madelung-energy correction. In defect calculations the point-charge approximation has clear limitations, but for systems with similar spatial arrangements of charge, the errors in the total energies due to the periodic boundary conditions will also be similar [19, 35]. Since relative ionization energies include the differences in these errors, they are often much more reliable than those obtained using formation energies, which are sensitive to errors in the band-gap.

The calculation of binding energies and electrical levels of large impurities and their aggregates involves an additional computational subtlety resulting from the affect of volume dilation on the elastic energy and band-gap. We showed previously that donors may appear artificially shallow if the strain effect on the band edges is not taken into account [21]. This means that the error bars on the electrical levels for large impurities are liable to be larger than for smaller species.

In the cases of N- and Te-pairs we have examined the cell size effects in more detail.

First, we compared the formation energy of substitutional impurities in a 216 atom cell with half the formation energy of two substitutional Te species at sixteenth neighbour sites. The difference is less than 10 meV for N and 0.2 eV for Te. Thus, for nitrogen pairs, the approximation that a 216 atom cell containing two substitutional N atoms at 16th neighbour sites represents non-interacting substitutional centres is clearly valid, but there may be an error of up to a few tenths of an eV for the largest species.

In addition, we investigated the role of cell size in the calculation of the relative locations of electrical transitions, since predicted levels have been shown to depend upon volume [21]. For nitrogen in 216 atom supercells, we find the donor levels of substitutional N and N-pairs relatively independent of volume relaxation (<0.1 eV). For Te-pairs the location of the donor level of the pair relative to that of a single substitutional Te is also largely independent of the volume (i.e. any volume relaxation effects approximately cancel when comparing these similar systems).

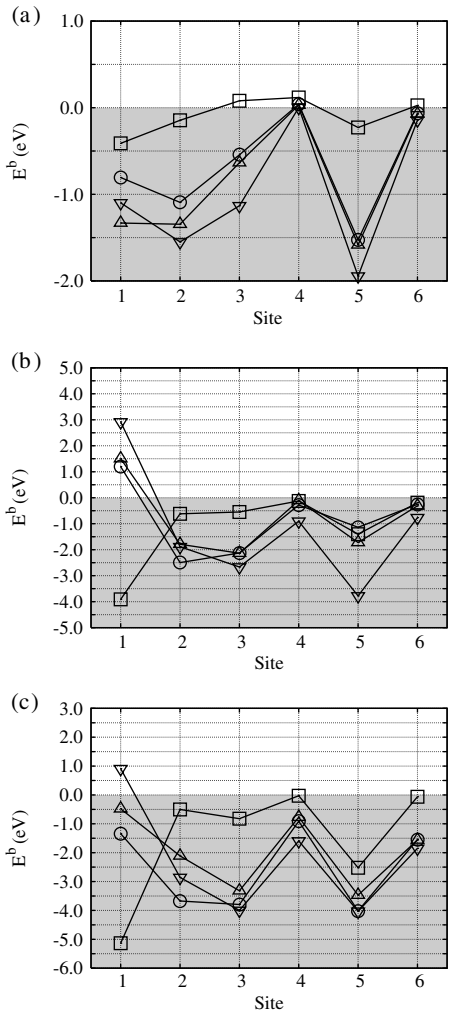

Figure 3. Binding energy of impurity pairs for sites shown in figure 2 relative to isolated substitutional centres (eV): (a) □—B, ○—Al, △—Ga, and ▽—In; (b) □—N, ○—P, △—As, and ▽—Sb; (c) □—O, ○—S, △—Se, and ▽—Te. The shaded area indicates bound systems.

Finally, we have also calculated the donor levels of Te_s and Te-pairs in a 512 atom super cell. Using phosphorus as a marker [35] the donor levels of Te_s and Te_2 in the 216 atom cell are $E_c - 1.3$ eV and $E_c - 0.2$ eV compared to $E_c - 1.3$ eV and $E_c - 0.1$ eV in the 512 atom cell. Thus, the smaller super cell is sufficient to model the properties of these centres.

Therefore, we conclude that although pairs of large impurities in the 216 atom supercell do give rise to volume effects, the impact upon binding energies and electrical properties is within the general accuracy of the method.

3. Results

3.1. Energetics

We first present in figure 3 the binding energies of impurity pairs as a function of separation in line with figure 2. Pairs of

group-IV species (Si, Ge and Sn) are found to be unbound and are not plotted.

We previously determined that vacancy–impurity complexes may be grouped broadly into two classes [22], and the same grouping is found for impurity pairing: the second-row elements (B, N, and O, squares in figure 3) show a preference for nearest-neighbour sites, whereas larger impurity species exhibit one or more lower energy, bound structures where the impurities are not in adjacent sites. In particular, group-III and chalcogen species, along with antimony favour fifth-neighbour sites, with phosphorus and arsenic favouring second- and third-neighbour sites, respectively. The focus of this study is in the interactions of the larger impurities, and we shall not discuss B, N, and O in any detail.

We note phosphorus and sulfur, both employed as n-type dopants, possess configurations more stable than two isolated donors, bound by 2.5 eV and 4.0 eV, respectively. These values are large in comparison to that of boron pairs, and the value for sulfur is comparable to that of nitrogen pairs. The high binding energies suggest that during high-temperature annealing, such as following ion implantation, pair formation is likely to proceed if the individual impurities can migrate. We also note that, in accord with the modest binding energy of boron pairs, other group-III acceptors are weakly bound.

All six sites analysed in this study represent bound configurations for different species. Site 1 is very stable for smaller impurities, such as boron and nitrogen. It also represents a stable site for the larger acceptor species, as well as sulfur and possibly Se. The larger donor impurities energetically prefer pairings where the sites are more distant. It is important to note that the profiles shown in figure 3 would not be predicted purely on the basis of isotropic elastic interactions, since impurities theoretically displace lattice volume as individual substitutional defects [22], and one would expect a repulsive elastic interaction.

To determine the origin of the attractive interactions that lead to bound impurity pairs we now present an exploration of the geometric and electronic structures.

3.2. Geometry

The bound structures are shown schematically in figure 4. In several cases more than one minimum in the energy is obtained for the fourth and fifth-shell configurations. Indeed, the structures depicted in figures 4(d)–(h) are often not obtained simply by substitution of carbon atoms in an ideal lattice: initial displacement of core atoms is essential, such as breaking the C–C bond in (e) and (g). We note that in structural relaxations it is rarely possible to demonstrate that one has obtained a global rather than local minimum in the energy. In an attempt to avoid any *shallow* minima in the energy surface, a relaxed structure may be perturbed by displacing atoms in random directions and re-optimising the geometry. By relaxing from several starting structures we aim to avoid trapping in a local minimum. For the structures discussed here, those taken to be the equilibrium geometries have been obtained from several different starting configurations.

In many cases, the structures indicate formation of bonds involving the two impurity sites and their carbon neighbours.

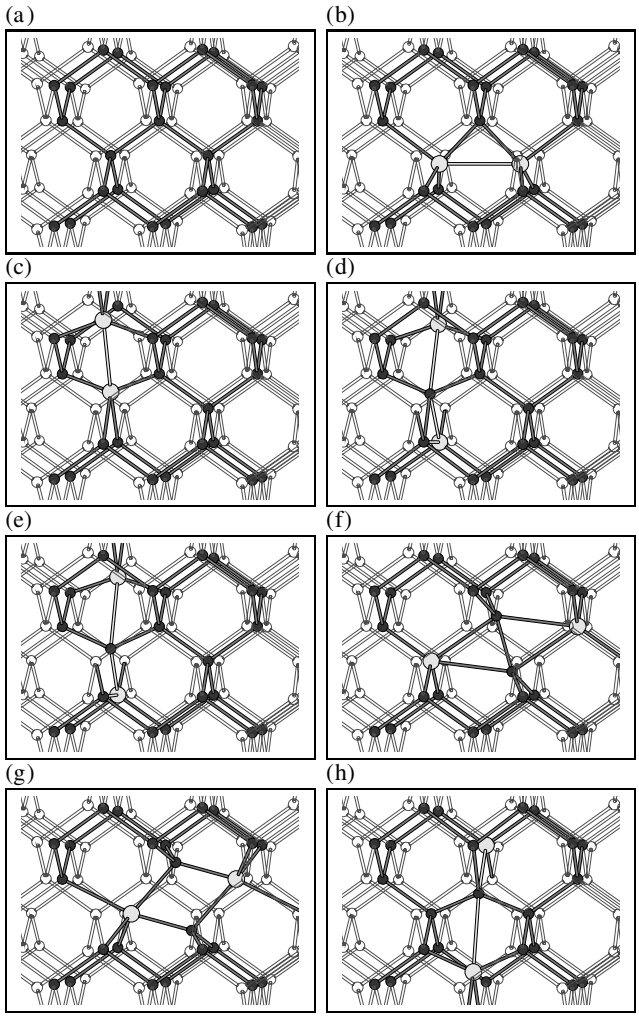

Figure 4. Schematic structure for (a) bulk diamond, (b) site 2, (c) site 3, (d) and (e) two reconstructions for site 4, (f) and (g) two reconstructions for site 5, and (h) site 6. Site numbering as in figure 2. In each plot, the horizontal is [110] and the vertical [001]. Dark and light atoms represent the host and impurity atoms, respectively, with surrounding carbon host shown as transparent to facilitate visualization of the structures.

The inter-impurity separations are mainly less than those of the comparable section of host material, as indicated by negative values of the fractional changes in inter-nuclear separations from the ideal lattice, ΔL_i, listed in table 1. There is a clear contrast with the large displacement moving the impurities away from one-another when they lie on adjacent sites (ΔL_1).

With the exception of nearest neighbours, both group-III acceptors and the iso-electronic, group-IV species exhibit small structural displacements and small or positive binding energies. The contrast seen for donors points to a binding involving the additional electrons for such pairs, due to formation of additional chemical bonds.

The geometric relaxations are most pronounced for donor pairs at sites 3 and 5. For example, the site 3 S–S distance is 29% shorter than the $[1\bar{1}3]a_0/4$ of pure diamond. In the case of site 5, the re-bonding is also rather clear: structure (f) involves a rotation of the central C–C bond from [111] to

Table 1. Structural and electrical parameters for impurity pairs. ΔL_i is the % change in inter-nuclear distance relative to bulk diamond for site i, figure 2. ΔE (eV) describes the ionization energy of the pairs relative to the dissociated impurities, as defined in the text. For comparison, the calculated values of ΔE for nearest-neighbour B, N and O pairs are 0.8, −2.2 and 0.0 eV, respectively. 'Site' indicates the value of i which possesses the lowest energy in the neutral charge state. Note, Si, Ge and Sn are lowest in energy in site 3 of the six examined, but these pairs are unbound relative to isolated impurities.

	Chemical species											
	Al	Ga	In	Si	Ge	Sn	P	As	Sb	S	Se	Te
Site	5	5	5	3	3	3	2	3	5	5	5	5
ΔL_1	45	35	43	27	28	40	32	34	47	45	49	54
ΔL_2	−2	−4	−2	2	3	5	−16	−11	−4	−24	−10	−2
ΔL_3	0	1	−3	0	0	0	−19	−16	−12	−29	−21	−15
ΔL_4	0	0	0	0	0	0	0	0	−4	−6	−9	−7
ΔL_5	0	1	0	1	2	2	−20	−19	−17	−5	−4	−16
ΔL_6	0	0	−1	0	0	0	−2	−5	−7	−6	−6	−5
ΔE	0.5	0.8	0.9	—	—	—	−1.4	−1.2	−2.5	−0.8	−0.4	0.3

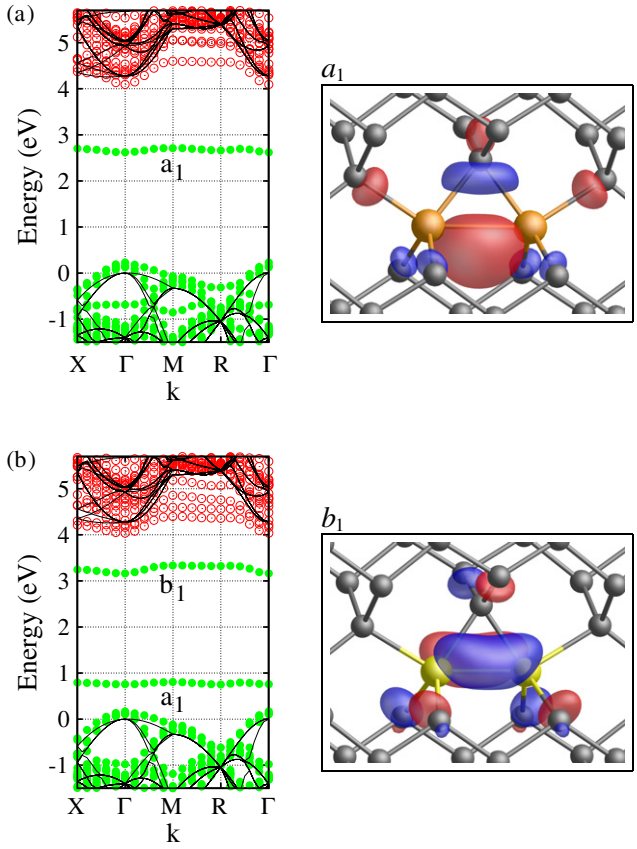

Figure 5. Band structure and wavefunction localization of the gap-levels for (a) P-pairs and (b) S-pairs at site 2 in figure 2. Kohn–Sham bands in the vicinity of the band-gap along high-symmetry directions of the first Brillouin-zone of a 216 atom supercell are plotted. Filled circles show occupied levels, and empty circles empty bands. Solid lines are the corresponding bands for a defect-free supercell, and the zero of energy is defined as the valence band top. In wavefunction plots, the horizontal is approximately [110] and the vertical [001], with impurities lighter in colour. The iso-surfaces are taken for $\psi^2 = 0.0225$ au^{-3}.

approximately 5° from [001], whereas in structure (g), the C–C bond previously lying between the impurities is broken. For example, for P and Sb in structure (g), the central carbon atoms are 38% and 54% further apart respectively, than a bulk C–C bond.

The fourth and sixth shells are stabilized for the chalcogens in a manner akin to site 3. However, in these cases, the re-bonding is between a donor and a *carbon* atom on the opposite side of a hexagonal ring. This relaxation provides space for the second chalcogen and lowers the total energy modestly. This relatively small effect is reflected in the binding energy of around 1 eV for the structure as shown in figure 3(c). The effect is also present for the pnictogens P, As, and Sb, but to a much reduced extent.

For the fourth and fifth shells, more than one stable structure has been obtained depending upon chemical composition. In general only one form is stable for a given impurity species, but in a few cases impurity pairs may exhibit both forms as minima in total energy.

For the pnictogens, the fourth-shell pairs, P and As favour figure 4(d) (both by 0.2 eV) and Sb favours (e) by 0.7 eV. For the fifth-neighbour pairs, P and As favour figure 4(g) by 1.0 eV, and Sb is only stable in this structure.

For the chalcogens, fourth-neighbour S- and Se-pairs favour figure 4(e) over (d) by 0.4 eV, whereas for Te, structure (d) is unstable. Te-pairs are bi-stable in the two fifth-neighbour structures, with that shown schematically in figure 4(f) ∼1 eV higher in energy than structure figure 4(g). However, the barrier for inter-conversion calculated using the NEB method with 13 points is around 0.1 eV, suggesting that (f) is practically unstable in this case. S- and Se-pairs are completely unstable in structure (g).

The propensity for greater geometric rearrangement for Sb and Te implies strain relaxation plays a role in the structure of impurity pairs, but the differences between pnictogens and chalcogens suggests an electronic effect. To shed further light on the re-bonding in the pairings, it is therefore necessary to examine the localization of the electronic states.

3.3. Electronic structure

Since different impurities are most stable in four of the seven configurations, and since site 3 is characteristic also of the reconstructions in sites 4 and 6, we examine configurations

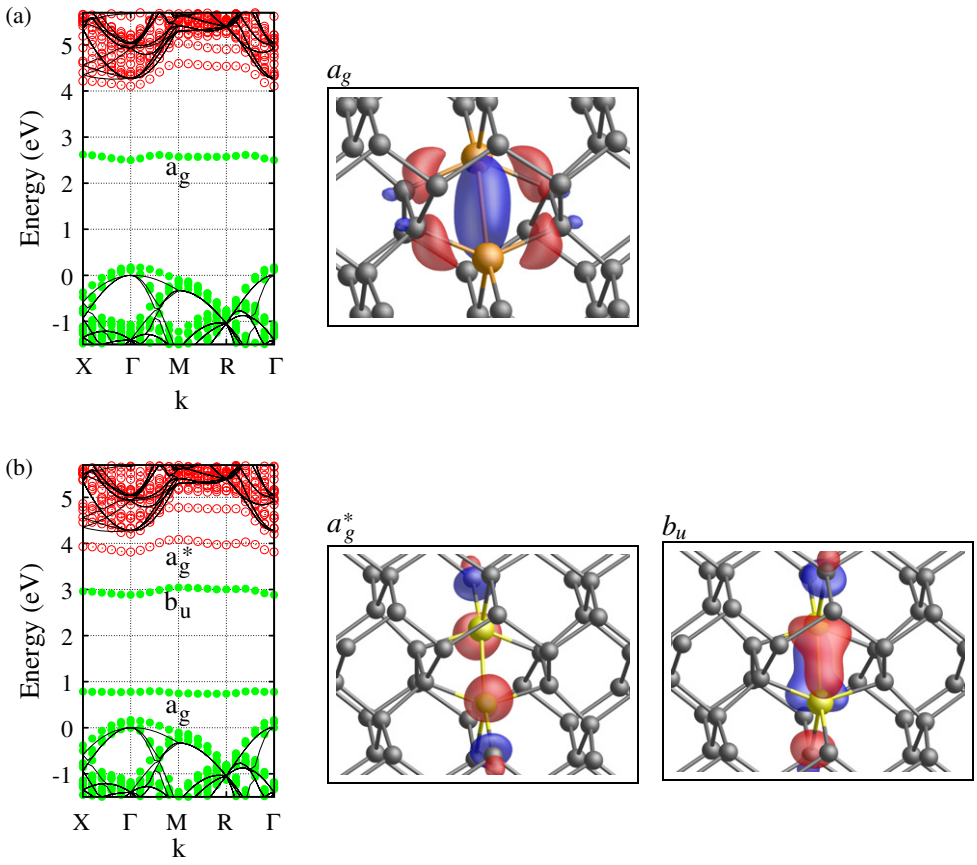

Figure 6. Band structures and localizations of the gap-levels for donor pairs in site 3 of figure 2. (a) P-pairs and (b) S-pairs. The Kohn–Sham bands, structures and iso-surfaces are plotted as in figure 5.

(b), (c), (f), and (g) in figure 4 in turn, starting with the C_{2v} symmetry second-neighbour pairs.

First, in passing we note that for group-III and iso-electronic impurities, there is no obvious re-bonding, although acceptor pairs possess empty gap-states localized in configurations which include a π-bonding character.

More importantly, as shown in figure 5 for the characteristic examples of P-and S-pairs, additional bond formation takes place. The band structure shows one(two) occupied bands in the band-gap for P(S) pairs. The location of the bands are lower in the band-gap for the second-neighbour pairs than the nearest-neighbour (not plotted) in line with the reduction in total energy and deepening of the donor level [26].

The localization of the band-gap levels (figure 5) clearly shows the re-bonding between the impurities. Both P and S possess a filled σ-bonding level (a_1 symmetry in the C_{2v} point group), and the S-pairs also have a π-bonding component (labelled b_1 in figure 5(b)). As one might expect, the a_1 band-gap level in the case of S-pairs closely resembles the a_1 level of the P-pair, and is therefore not plotted.

Third-neighbour, C_{2h} symmetry P- and S-pairs are presented in figure 6. Again, in the case of P, the occupied a_g gap-level shows σ-bonding between the impurities. A comparable level is also present low in the band-gap for sulfur pairs, and the b_u highest occupied level is made up from a π-bonding component. It is the combination of these that leads to the dramatic 29% shortening of the S–S distance relative to the ideal host. For the S-pair, there is also an empty a_g^* band-gap level chiefly made up from an anti-bonding combination of p-orbitals on the S atoms, and sp-hybrids on the two equivalent nearest carbon neighbours. Dipole selection rules allow for optical transitions between the b_u and a_g^* levels.

Qualitatively similar reconstructions are present in the fourth and sixth-neighbour pairs (figures 4(d), (e) and (h)). However, since the formation of the reconstruction involves the distortion of C–C bonds in these cases the stabilization energy is lessened relative to third-nearest neighbour pairs.

Finally, figure 7 shows the case of the fifth-shell pairs. In this case there are two different energy minima. Whether a particular species takes one form or the other is a balance between the energy saved in the electronic interactions leading to bond formation, and the geometric relaxation concomitant with the atomic size.

We note that as with the third-shell pairing, the presence of filled and empty band-gap levels provides a mechanism for localized optical transitions for S-pairs.

Although the preceding analysis focuses upon P and S, qualitatively similar results are for the other pnictogens and chalcogens.

The band structures shown in figures 5–7 are indicative of deep donor activity relative to the levels of the isolated donor species. For instance, the filled band around 2 eV below E_c

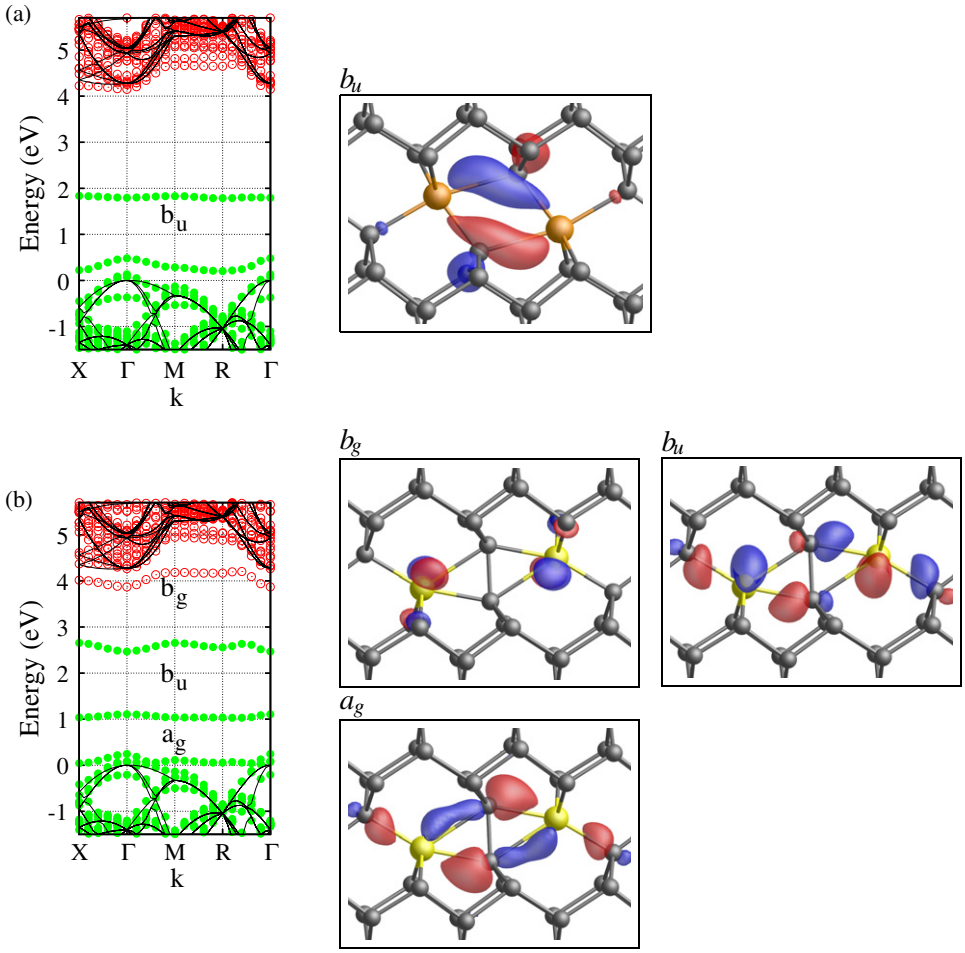

Figure 7. Band structures and localizations of the gap-levels for donor pairs in site 5 of figure 2. (a) P-pairs and (b) S-pairs. The Kohn–Sham bands, structures and iso-surfaces are plotted as in figure 5.

in figure 5(a) is much deeper than that of isolated phosphorus donors. However, to put the effect on a more quantitative footing we have calculated the change in the location of the first ionization of both acceptor and donor species for the most stable arrangement of each pairing (i.e. fifth-neighbour pairs with the exception of P and As which are second and third neighbours, respectively). ΔE in table 1 is the location of the calculated donor or acceptor level for the most stable form of paired complexes relative to that calculated for an individual substitutional donor or acceptor. For example, the donor level of the most stable phosphorus pair is calculated to lie 1.4 eV lower in energy than an isolated phosphorus donor. In calculating the *differences* in donor and acceptor levels, the well known short-comings for calculations involving charged, periodic systems are somewhat mitigated [35].

For the group-III species other than B, the values are positive (that is the pairs are deeper acceptors than the isolated impurities) by 0.5–0.9 eV. Given that these species are already deep acceptors [19], so are the acceptor pairs. For boron, the pairing deactivates the shallow acceptors [39, 40].

For the pnictogens, the pairing also pushes the donor levels deeper into the band-gap (since the donor level is referenced to the conduction band, a negative value for ΔE represents an increase in ionization energy for conduction). In particular, for phosphorus pairs in the most energetically favourable pairing (site 2 in figure 2) the activation energy for promotion of an electron to the conduction band increases by 1.4 eV. Using the experimental value for the P_s donor as a reference, this places the donor level of the P-pair at $E_c - 2.0$ eV, and therefore for every pair formed, two P donors are deactivated.

The picture is similar for the chalcogens. In the case of the sulfur donor, pairing in the most stable, fifth-shell sites pushes the donor level around 0.8 eV deeper into the band-gap, so that even if S_s possesses a useful donor level, pairing will also result in deactivation in this case.

4. Discussion and conclusions

We have studied the effect of impurity pairs in diamond, and find the following key results.

(i) Large donor and acceptor species are bound in pairs, despite individually exerting a compressive strain on the surrounding material.
(ii) In the case of donor species, nearby pairs interact *chemically*, forming strong bonds.
(iii) The pairing of impurities in this fashion does not result in repulsive interaction of defect levels (such as suggested by

figure 1 and [12, 24]) but in all cases we have examined, with the possible exception of Te–Te complexes, the levels are hyper-deep and highly localized.

(iv) With the exception of iso-electronic centres which are optically inactive, the presence of impurity pairs leads to optical transitions involving one or both band edges. Such transitions would be expected to lead to rather broad absorption or emission. In addition, particularly in the case of chalcogen pairs, there are both filled and empty levels localized in the vicinity of the impurities, corresponding to rather sharp optical transitions.

We note that similar direct interaction of n-type impurities has previously been suggested for doped silicon [41, 42], involving chemical reconstruction, lattice vacancies and self-interstitials. The current presentation closely matches the suggestion that proximity of dopants, perhaps due to high dopant concentrations, may lead to varying degrees of deactivation.

We also note that in early luminescence experiments on phosphorus-doped diamond, a broad band centred around 1.9 eV was observed [43, 44]. Although this may be related to the incorporation of phosphorus–vacancy pairs [45] this is also close to the donor level of the P-pairs, which would also be expected to yield rather broad luminescence. In contrast, the potential internal transitions that theoretically exist for chalcogen pairs would be expected to be sharp, providing a mechanism for optical detection of such complexes.

Finally, we briefly comment upon the thermal stability of dopant pairs. Where dopants are introduced by implantation and the material subsequently annealed to high temperatures, the likelihood for formation of impurity pairs also depends in a non-trivial fashion upon the presence of lattice damage, the migration mechanism and barriers, the capture cross-section for pair formation, and the free-binding-energy at the annealing temperatures. In the case of S-pairs, the zero-temperature binding energy is around that of nitrogen pairs which remain stable to 2000 °C [46], so it seems reasonable to expect sulfur pairs to be stable during post-implantation annealing. Therefore, impurity aggregation in doped and annealed material cannot be excluded for a wide range of donor species, although a more detailed thermodynamical model is required. For iso-electronic species such as Si, and group-III species such as Al and Ga, any propensity for pair formation is absent or much reduced relative to that indicated for the pairing of the pnictogen and chalcogen species examined in this report.

Acknowledgment

We gratefully acknowledge the EPSRC for funding.

References

[1] Crowther P A, Dean P J and Sherman W F 1967 *Phys. Rev.* **154** 772–85
[2] Lagrange J P, Deneuville A and Gheeraert E 1998 *Diamond Relat. Mater.* **7** 1390–3
[3] Farrer R 1969 *Solid State Commun.* **7** 685
[4] Gheeraert E, Koizumi S, Teraji T and Kanda H 2000 *Solid State Commun.* **113** 577–80
[5] Okushi H 2001 *Diamond Relat. Mater.* **10** 281–8
[6] Hasegawa M, Takeuchi D, Yamanaka S, Ogura M, Watanabe H, Kobayashi N, Okushi H and Kajimura K 1999 *Japan. J. Appl. Phys.* 2 **38** L1519–22
[7] Horiuchi K, Kawamura A, Ide T, Ishikura T, Takamura K and Yamashita S 2001 *Japan. J. Appl. Phys.* 2 **40** L275–8
[8] Trajkov E, Prawer S, Butler J E and Hearne S M 2005 *J. Appl. Phys.* **98** 023704
[9] Koeck F A M and Nemanich R J 2005 *Diamond Relat. Mater.* **14** 2051–4
[10] Miyazaki T and Okushi H 2001 *Diamond Relat. Mater.* **10** 449–52
[11] Nishimatsu T, Katayama-Yoshida H and Orita N 2001 *Physica* B **302/303** 149–54
[12] Katayama-Yoshida H, Nishimatsu T, Yamamoto T and Orita N 2001 *J. Phys.: Condens. Matter* **13** 8901–14
[13] Nishimatsu T, Katayama-Yoshida H and Orita N 2002 *Japan. J. Appl. Phys.* 1 **41** 1952–62
[14] Wang L G and Zunger A 2002 *Phys. Rev.* B **66** 161202(R)
[15] Miyazaki T 2002 *Phys. Status Solidi* a **193** 395–408
[16] Sque S J, Jones R, Goss J P and Briddon P R 2003 *Physica* B **340–342** 80–3
[17] Sque S J, Jones R, Goss J P and Briddon P R 2004 *Phys. Rev. Lett.* **92** 017402
[18] Lombardi E B, Mainwood A and Osuch K 2004 *Phys. Rev.* B **70** 205201
[19] Goss J P, Briddon P R, Sque S J and Jones R 2004 *Diamond Relat. Mater.* **13** 684–90
[20] Cai Y, Zhang T, Anderson A B, Angus J C, Kostadinov L N and Albu T V 2006 *Diamond Relat. Mater.* **15** 1868–77
[21] Goss J P, Briddon P R and Eyre R J 2006 *Phys. Rev.* B **74** 245217
[22] Goss J P, Briddon P R, Rayson M J, Sque S J and Jones R 2005 *Phys. Rev.* B **72** 035214
[23] Yu B D, Miyamoto Y and Sugino O 2000 *Appl. Phys. Lett.* **76** 976–8
[24] Segev D and Wei SH 2003 *Phys. Rev. Lett.* **91** 126406
[25] Miyazaki T, Okushi H and Uda T 2002 *Phys. Rev. Lett.* **88** 066402
[26] Eyre R J, Goss J P, Briddon P R and Wardle M G 2007 *Phys. Status Solidi* a **204** 2971–7
[27] Coutinho J, Torres V J B, Jones R and Briddon P R 2003 *Phys. Rev.* B **67** 035205
[28] Davies G 1976 *J. Phys. C: Solid State Phys.* **9** L537–42
[29] Jones R and Briddon P R 1998 *Semiconductors and Semimetals* (*The Ab Initio Cluster Method and the Dynamics of Defects in Semiconductors* vol 51A) (Boston: Academic) chapter 6
[30] Perdew J P and Wang Y 1992 *Phys. Rev.* B **45** 13244–9
[31] Monkhorst H J and Pack J D 1976 *Phys. Rev.* B **13** 5188–92
[32] Hartwigsen C, Goedecker S and Hutter J 1998 *Phys. Rev.* B **58** 3641–62
[33] Henkelman G, Uberuaga B P and Jónsson H 2000 *J. Chem. Phys.* **113** 9901–4
[34] Henkelman G and Jónsson H 2000 *J. Chem. Phys.* **113** 9978–85
[35] Goss J P, Shaw M J and Briddon P R 2007 *Theory of Defects in Semiconductors* (*Topics in Applied Physics* vol 104) ed D A Drabold and S K Estreicher (Berlin/Heidelberg: Springer) pp 69–94
[36] Liberman D A 2000 *Phys. Rev.* B **62** 6851–3
[37] Sze S M 1981 *Physics of Semiconductor Devices* 2nd edn (New York: Wiley–Interscience)
[38] Makov G and Payne M C 1995 *Phys. Rev.* B **51** 4014–122
[39] Goss J P and Briddon P R 2006 *Phys. Rev.* B **73** 085204
[40] Bourgeois E, Bustarret E, Achatz P, Omnés F and Blase X 2006 *Phys. Rev.* B **74** 094509
[41] Citrin P H, Voyles P M, Chadi D J and Muller D A 2003 *Physica* B **340–342** 784–9

[42] Voyles P M, Chadi D J, Citrin P H, Muller D A, Grazul J L, Northrup P A and Gossmann H J L 2003 *Phys. Rev. Lett.* **91** 125505
[43] Cao G Z, Driessen F A J, Bauhuis G J, Giling L J and Alkemade P F A 1995 *J. Appl. Phys.* **78** 3125–31
[44] te Nijenhuis J, Olsthoorn S M, van Enckevort W J P and Giling L J 1997 *J. Appl. Phys.* **82** 419–22
[45] Jones R, Lowther J E and Goss J 1996 *Appl. Phys. Lett.* **69** 2489–91
[46] Evans T and Qi Z 1982 *Proc. R. Soc.* A **381** 159–78